SONIC BOOM PREDICTION FOR THE LANGLEY MACH 2 LOW-BOOM CONFIGURATION

Michael D. Madson
NASA Ames Research Center
Moffett Field, CA

SUMMARY

Sonic boom pressure signatures and aerodynamic force data for the Langley Mach 2 low sonic boom configuration were computed using the TranAir full-potential code. A solution-adaptive Cartesian grid scheme is utilized to compute off-body flow field data. Computations were performed with and without nacelles at several angles of attack. Force and moment data were computed to measure nacelle effects on the aerodynamic characteristics and sonic boom footprints of the model. Pressure signatures were computed both on and off ground-track. Near-field pressure signature computations on ground-track were in good agreement with experimental data. Computed off ground-track signatures showed that maximum pressure peaks were located off ground-track and were significantly higher than the signatures on ground-track. Bow shocks from the nacelle inlets increased lift and drag, and also increased the magnitude of the maximum pressure both on and off ground-track.

INTRODUCTION

The High Speed Research Program (HSRP) has been initiated with the goal of designing and testing a supersonic commercial transport aircraft with acceptable aerodynamic qualities, acceptable emission levels and, if possible, sonic boom signatures that would permit supersonic flight over land. It is generally considered that a signature with an initial overpressure of 0.5-1.0 psf and a noise level of 72 DbA or less on the ground would be acceptable, although no firm definition of acceptability has been established.

In support of the HSRP program, a conceptual low-boom aircraft geometry was designed at NASA Langley using a process that integrates low boom design and aerodynamic performance methods (ref. 1). A drawing of the Mach 2 conceptual model is shown in figure 1. This configuration was designed to produce a "flat-top" pressure signature with a maximum overpressure of slightly less than 1 psf on the ground. Wind tunnel data were obtained at $M_\infty=2.0$ and 2.5 for several values of C_N. Pressure signatures were measured on ground-track at several distances from the model. Drag data were not measured during the tests.

There are several efforts ongoing to calculate accurate near- and far-field pressure signatures (refs. 2-6) and to design low sonic boom aircraft (refs. 1,7). These efforts utilize different approaches to the computation of offbody pressure signatures and the extrapolation of the signatures to the ground. Significant use is still being made of the Whitham method (ref. 8), a quasi-linear technique introduced in 1952. Most of the current efforts are focused on the application of computational fluid dynamics (CFD) codes to the prob-

157

lem. The basic approach is to compute pressure signatures at a distance from the model which is far enough for the model effects to be considered axisymmetric (typically anywhere from 0.5 to 1.0 body lengths), then extrapolating the signature to the far-field using a conventional technique such as the Whitham method. In this way, lift and equivalent area are taken into account in the computation. Lift calculations from non-linear CFD codes are more accurate than those from the linear methods which were originally used.

For this paper, the TranAir code (refs. 9,10) was used to compute force data for the Mach 2 model, as well as offbody pressure signatures for sonic boom calculation. TranAir solves the non-linear full-potential equation for subsonic, transonic, and supersonic flow about arbitrary configurations. The surface geometry is defined by networks of surface panels in the same manner as linear-potential panel methods. Also, wake sheets must be defined from the trailing edges of lifting surfaces to enforce the Kutta condition. The flow-field is defined as a rectangular array of Cartesian grid points, within which is embedded the surface definition of the configuration. The decoupling of the surface and grid definition processes allows the user to routinely analyze very complex and realistic models. TranAir was developed to compute the aerodynamics of complex configurations in the three flow regimes (refs. 11-18), but its solution-adaptive flow-field grid capability makes it ideal for computing offbody pressure signatures for sonic boom analysis and design. A validation of TranAir's ability to accurately compute offbody pressure signatures was recently completed (ref. 6).

Computational results for the Mach 2 model with and without flow-through nacelles were obtained at $M_\infty=2.0$ for angles of attack ranging from -1 to 6 degrees. Pressure signatures were calculated near the model and extrapolated to distances at which experimental data were measured using a quasi-linear extrapolation technique (ref. 19). Good agreement was found between experiment and computation for the Mach 2 model without nacelles. Experimental data with open nacelles showed an unexpected spike in the pressure signature. TranAir results for the cases of flow-through nacelles and blocked nacelles verified that the spike was caused by unstarted nacelles in the tunnel. Also verified was the existence of off ground-track signatures which had maximum pressures exceeding those which exist on ground-track. This phenomenon was first predicted by Siclari (ref. 3).

WIND TUNNEL MODEL AND TEST PROCEDURE

The Mach 2 model was designed to produce a low sonic boom signature on the ground with the following constraints: A cruise Mach number of 2.0, a cruising altitude of 55,000 ft, a beginning-cruise weight of 550,000 lb, a range of 5000 nm, and a length of approximately 300 ft. The goal of the design was to produce a "flat-top" signature on the ground, in which there is an initial shock of approximately 1 psf, which remains constant until an expansion from the aft end of the model is encountered. The final design for the conceptual model is 313 ft long with a wing span of 160 ft, a wing dihedral of 4.6°, a "platypus" nose with a blended wing root, and a supersonic outboard leading edge. Four circular nacelles approximately 34 ft long are placed near the inboard trailing edge to minimize volume and interference effects. A wind tunnel model of the Mach 2 configuration was manufactured based on the final design. The

length of the wind tunnel model is approximately 12 in, with an integrated sting and an external strain gauge on the sting for normal force and moment measurement.

Wind tunnel tests of the Mach 2 model were conducted in the NASA Ames 9 ft by 7 ft Supersonic Wind Tunnel and the NASA Langley 4 ft Supersonic Wind Tunnel. A photograph of the Mach 2 model installed in the test section of the Ames 9 ft by 7 ft tunnel is shown in figure 2. Note that the model is installed in a wing-vertical attitude in the tunnel. Pressure signatures in the wind tunnel are obtained by two static pressure probes mounted along the side wall of the tunnel which faces the underside of the model. One probe is a reference (seen in the lower left corner of figure 2) placed out of the zone of influence of the model, and away from the model centerline to keep the probe shock from interfering with the flow along the centerline of the model. The overpressure probe is placed along the model centerline, and within the zone of influence of the model (seen in the upper left portion of figure 2). The probe positions remain constant, and the the model is traversed along the flow axis by a motor-driven shaft mounted on the support assembly as seen at the far right edge of figure 2, downstream of the angle of attack mechanism. The measurement of the pressure signature begins with the model in the downstream position in the test section, and data points are taken as the model is traversed in the upstream direction. The distance between the model and the overpressure probe is increased or decreased by moving the motor-driven horizontal strut on which the model is attached. Experimental pressure signatures were obtained at distances ranging from 0.65 to 5.3 body lengths from the model.

DISCUSSION OF COMPUTATIONAL METHOD

TranAir solves the non-linear full-potential equation for subsonic, transonic, and supersonic flow about arbitrary configurations. The theoretical aspects and the solution method used by TranAir have been reported (refs. 9,20-23) and will not be addressed here. Instead, a description of the code from an applications standpoint is presented.

The surface definition of the configuration being analyzed is defined by networks of surface panels, in the same manner as panel method codes. The surface definition of the Mach 2 model with flow-through nacelles is shown in figure 3. Approximately 10,300 surface panels were used to define this configuration, which were organized into 93 networks. Wakes from the wing trailing edge, nacelle exits, and fuselage base were defined by 29 networks consisting of a total of 620 wake panels. Removal of the nacelles reduced the number of surface panels to about 7,500 (31 networks), and the number of wake panels to 164 (8 networks). Unlike panel methods, the number of surface panels defining the configuration has a small effect on the CPU time required to obtain the solution. Instead, factors including the freestream Mach number, the number of grids for which the solution is computed, the number of flow-field grid points for each grid, and whether a solution-adaptive or multi-grid scheme is chosen to solve the problem drive the CPU time requirement.

The flow field is defined by a rectangular array of Cartesian grid points. This method of surface-grid and flow-field definition avoids the use of surface-conforming flow-field grids, and allows for the routine set-up and analysis of arbitrary and complex aerodynamic configurations. For transonic flow problems, the Cartesian grid need only be large enough to encompass any supercritical flow regions. The code solves the Prandtl-Glauert equation around the outer set of grid boxes, thus the flow need merely be linear, not unperturbed, at the grid borders. For fully supersonic problems, however, the grid must extend far enough away that reflected shocks from the grid boundaries do not intersect the configuration surface. Experience has suggested that for pressure signature measurements away from the body, grid boundaries be established as far as two body lengths below and behind the model. A large global grid tends to improve the quality of the solution near the boundaries of the grid, and reduces the percentage volume of the global grid which must be highly refined for the offbody computations.

The solution-adaptive grid-refinement capability within TranAir is critical to the accurate prediction of shocks away from the surface of the model. For sonic boom calculations, a relatively dense grid must be maintained to significant distances from the body to calculate an accurate pressure signature. The initially uniform flow-field grid is adaptively refined based on local flow conditions. In regions where shocks and large velocity gradients exist, the grid will be successively refined until adequate resolution is obtained. A refinement consists of dividing a grid box into eight geometrically similar boxes. An oct-tree data structure is used to efficiently store and access pertinent information regarding the refined grid.

The user may exert significant influence on the refinement process. One or more hexahedral regions may be defined within the global grid. Maximum and minimum refinement levels within these regions may be specified by the user. The refinement controls within this region supersede the globally specified refinement criteria. This allows for the definition of regions of "interest" or "disinterest," depending on whether the user specifies additional refinement or limits the refinement within the volume. Examples of regions that might be defined include a region enclosing a wing leading-edge to increase grid resolution for a careful drag study and a region enclosing the empennage limiting the refinement so that more grid points are available for a wing/nacelle integration study. For the case of sonic boom prediction, a user-specified region underneath the aircraft is usually required to obtain accurate offbody pressure signatures at distances up to one body length from the surface.

Figure 4 provides an example of a TranAir solution adaptive grid for the Mach 2 model. Figure 4(a) shows a 2-D cut along the centerline of the model. Figure 4(b) shows a cut through the wing and the centerline of the inboard nacelle. These slices clearly display the solution-adaptive capability of the code, as well as the relationship between the flow-field grid boxes and the surface geometry. A typical solution for the Mach 2 model used 8MW of central memory, approximately 200MW of temporary disk space, and about 2 CPU hours on a Cray Y-MP.

Flow quantities from TranAir are available both on the surface and in the flow-field. A graphics program has been written (ref. 10) that allows for the inspection of the non-uniform grids generated by TranAir. Another graphics program has been modified (ref. 24) to read TranAir geometry information and

aerodynamic quantities on the surface of the configuration. The program displays wire mesh and shaded-surface renditions of the model and flow quantities such as velocity, pressure coefficient, or local Mach number on the configuration surface.

RESULTS

TranAir force data computed for a series of angles of attack for the nacelle-on and nacelle-off cases are presented in figure 5. The presence of the nacelles increased C_L by approximately 0.005 due to the positive pressures on the lower surface induced by the nacelles. This increase in lift may be slightly under-predicted because of a violation of the isentropic assumption near the inlet bow-shock. The nacelles caused an increase in drag of about 20 counts. The pitching moment was nearly identical for the two cases. Wind tunnel tests were conducted both with and without nacelles. Values of C_N and C_M were measured but drag data was not measured.

TranAir predictions for L/D for the nacelle-on and nacelle-off cases are shown in figure 6. Viscosity is neglected for these calculations, so the L/D values shown in figure 6 are significantly higher than what would be measured in a wind tunnel test. The presence of the nacelles lowers the maximum L/D for the configuration by 30% relative to the nacelle-off case. The angle of attack at which the maximum L/D occurs is about 0.25° for the nacelle-off case, and about 0.75° with the nacelles on.

The Mach contours on the lower surface of the Mach 2 model without nacelles are shown in figure 7. For this case, $M_\infty=2.0$ and $C_N=0.05$. Two prominent features appear in this figure. The first is the large expansion region along the aft of the fuselage and the trailing edge of the wing. Also apparent is the large compression region along the leading edge of the outboard wing section. The compression is caused by the supersonic leading edge along the outboard wing section. The effect of this compression on the sonic boom footprint of the model will be discussed later in this section.

The Mach contours presented in figure 8, also for $M_\infty=2.0$ and $C_N=0.05$, show the effect of the nacelles on the surface Mach numbers for the Mach 2 model. Significant compression regions are introduced by the nacelles on the lower surface of the wing, causing an increase in C_L relative to the nacelle-off case. The complex nature of the flow on the underside of the model due to the presence of the nacelles is evident in the figure. Bow shocks in front of the inlets can be seen to impinge on each other, and the neighboring nacelle. The effect of the inlet bow shock on the fuselage is evident. The bow shocks also weaken the expansion along the trailing edge of the wing.

A plot of $\Delta p/p_\infty$ for a nacelle-off run at $M_\infty=2.0$ and $C_N=0.05$ is shown in figure 9. The signature was measured below the model at an h/L (distance from model in the centerplane normalized by the model length) of 0.651. The flat top signature generated by the first 60% of the model is a desirable low-boom characteristic, and was a goal of the design process. The computational results were obtained by sampling the flow-field at h/L=0.20 and extrapolating to the h/L distance at which tunnel data were measured. The

computational results are in good agreement with experiment with two exceptions. First, the magnitude of the nose overpressure is low compared with experimental data. The strength of the nose shock dissipates very quickly, and better results are obtained from measurements closer to the body. The grid structure shown in figure 4(a) shows that the flow-field grid is highly refined near the nose, but becomes relatively coarse at h/L=0.20. Second, the expansion along the aft portion of the fuselage is interrupted by a weak compression of unknown origin. It is felt than an imperfection in the wind tunnel model may have caused the weak shock.

Tests conducted with the nacelles installed yielded a significantly different pressure-signature aft of the flat-top region (figure 10). A large shock appears in the data which was not anticipated during the design process. A closer look at the nacelle geometry (figure 3) shows that the leading edge is blunt, tapering down to a constant-diameter internal duct. The Mach contours from figure 8 clearly show that bow shocks are present in front of the nacelle inlets which affect the pressure signature at the centerline of the model. The computed magnitude of the pressure peak at the centerline caused by the nacelles was quite low in comparison with experiment. It was felt that the magnitude of the experimental pressure peak may have been caused by unstarted nacelle inlets.

A numerical study was undertaken to verify the cause of the strong shock in the experimental pressure signature. Two models were analyzed in which the nacelles were modeled as flow-through, and with blocked inlets. For these cases, $M_\infty=2.0$ and $C_N=0.07$. TranAir pressure signature measurements are compared with experimental data in figure 10. Again, TranAir results were computed at h/L=0.20 and extrapolated to h/L=0.651, where experimental data were measured. These results show that the cause of the large shock in the signature is most likely due to flow blockage at the nacelle inlets. The flow-through case also has a significant compression along the model centerplane due to shocks from the inlets, though much lower in magnitude. TranAir predicts the shape of the pressure signature well, but underpredicts the magnitude of the compression at the centerplane caused by the bow shock from the nacelle inlets for the blocked-nacelle case. The smallest flow-field grid box in the vicinity of the nacelles measures about 0.03 in. in length in all three directions, which is equivalent to almost 400 grid points along the length of the body. However, this only corresponds to three boxes across the nacelle inside diameter, and less than seven across the outside diameter (figure 4a). This type of resolution will permit an adequate estimate of the flow features at the inlet to compute global effects reasonably well, but will not resolve the bow shock strength well enough to compute its proper contribution to the pressure signature in the flow field.

Two factors in predicting offbody pressure signatures for a complex configuration need to be balanced: the fineness of the grid required to accurately capture flow-field features away from the body, and the distance from the model at which data should be calculated in order to assure that the three-dimensional effects have been incorporated into the pressure signature. In making a computational prediction, these two factors may need to be compromised in order to obtain the most accurate computational solution within both code and machine limitations.

A series of shocks aft of the model appear in the measured data shown in figure 10. These are caused by the presence of the model-supporting hardware downstream. These smaller shocks eventually coalesce into one very large shock which begins to overtake the model tail shock. The downstream hardware is not included in the TranAir analysis.

Previous results from CFD (ref. 3) indicated that the maximum overpressure for the Mach 2 model does not exist on ground-track. Instead, peak overpressures are found off ground-track. Experimental data for the Mach 2 model have verified this phenomenon. The surface contours in figures 7 and 8 show large compressions along the outboard wing leading edge indicating peak pressures in that region. A series of TranAir runs were made for the Mach 2 model with and without nacelles to evaluate the sonic boom footprints generated by the two configurations. Figure 11 shows the sonic boom footprints (Mach contours) at 0.20 body lengths from the Mach 2 model without nacelles for M_∞=2.0 and angles of attack ranging from 1 to 5 degrees. The planform of the model is shown semi-transparent above the plane for visual reference. The sonic boom footprints for the model with nacelles are shown in figure 12. For both cases it is seen that a strong compression followed by a large expansion exists off ground-track. The compression is caused in large part by the supersonic outboard leading edge. The expansion originates at a point along the fuselage where the diameter begins tapering down, and propogates along the trailing edge of the wing. Plots of $\Delta p/p_\infty$ on and off ground-track for the Mach 2 model without nacelles are shown in figure 13 for C_N=0.08 at h/L=0.20. The corresponding plots for the Mach 2 model with nacelles are presented in figure 14. The off ground-track location is represented in degrees from the model centerline at 0.20 body lengths from the model. Comparing the two cases shows several differences in the signatures caused by the presence of the nacelles. The peak pressure on ground-track was increased significantly by the impinging bow shock from the inboard inlet. Peak pressures at all ground-track stations were increased to some degree by the nacelles. The expansion from the wing trailing edge was reduced slightly by the presence of the nacelles. This was caused by the interruption of the expansion from the fuselage and wing trailing edge by the inlet bow shocks.

CONCLUSIONS

The TranAir full-potential code, using a solution-adaptive grid refinement procedure on an unstructured Cartesian mesh, was used to compute the aerodynamics and the offbody pressure signatures of the NASA Langley Mach 2 model, which was designed to produce a flat-top pressure signature on the ground for low boom considerations. Computational pressure signatures were calculated by combining TranAir offbody results with a quasi-linear extrapolation technique. Comparisons with experimental data on ground-track were in good agreement. The front half of the signature shows the flat-top that was one of the design goals. The presence of the nacelles causes several adverse effects. There are strong bow shocks from the nacelle inlets at M_∞=2.0 which cause a strong compression in the pressure signature. TranAir runs with flow-through nacelles and blocked-inlets showed that the nacelles of the wind tunnel model were probably blocked. TranAir results showed a bow shock of significant strength for the flow-through nacelles which cause unexpected compressions in the pressure signatures both on and off ground-track. Off ground-track

pressure signature computations show that the maximum pressures in the sonic boom footprint for the Mach 2 model occur off ground track due in large part to the supersonic outboard leading edge. This is true with and without nacelles, although the bow shock from the nacelles increase the maximum pressure peaks relative to the nacelles-off case. To be a viable model, design modifications to the Mach 2 model will be necessary. The outboard leading edge must be made subsonic to alleviate the large compressions off ground-track. Also, the nacelles must be more carefully defined to minimize or avoid large bow shocks, which impacts peak pressures both on and off ground track.

REFERENCES

1.   Mack, Robert J.; and Needleman, Kathy E.: *A Methodology for Designing Aircraft to Low Sonic Boom Constraints*. NASA TM-4246, 1991.

2.   Cheung, Samson H.; Edwards, Thomas A.; and Lawrence, Scott L.: *Application of CFD to Sonic Boom Near and Mid Flow-Field Prediction*. AIAA Paper 90-3999, 1990.

3.   Siclari, Michael J.; and Darden, Christine M.: *CFD Predictions of the Near-Field Sonic Boom Environment for Two Low Boom HSCT Configurations*. AIAA Paper 91-1631, 1991.

4.   Page, Juliet A.; and Plotkin, Kenneth J.: *An Efficient Method for Incorporating Computational Fluid Dynamics Into Sonic Boom Prediction*. AIAA Paper 91-3275, 1991.

5.   Cliff, Susan E.; and Thomas, Scott D.: *Euler/Experiment Correlations of Sonic Boom Pressure Signatures*. AIAA Paper 91-3276, 1991.

6.   Madson, Michael D.: *Sonic Boom Predictions for Three Generic Models Using a Solution-Adaptive Full-Potential Code*. AIAA Paper 91-3278, 1991.

7.   Haglund, George T.: *HSCT Designs for Reduced Sonic Boom*. AIAA Paper 91-3103, 1991.

8.   Whitham, G. B.: The Flow Pattern of a Supersonic Projectile. *Comm. Pure & Appl. Math.*, Vol. V, No. 3, Aug. 1952, pp. 301-348.

9.   Johnson, Forrester T.; et. al.: *TRANAIR: A Full-Potential, Solution-Adaptive Rectangular Grid Code for Predicting Subsonic, Transonic, and Supersonic Flows About Arbitrary Configurations (Theory Document)*. NASA CR-4348, 1991.

10.   Johnson, Forrester T.; et. al.: *TRANAIR: A Full-Potential, Solution-Adaptive Rectangular Grid Code for Predicting Subsonic, Transonic, and Supersonic Flows About Arbitrary Configurations (User Guide)*. NASA CR-4349, 1991.

11.   Erickson, Larry L.; Madson, Michael D.; and Woo, Alex C.: Application of the TranAir Full-Potential Code to the F-16A. *AIAA J. Aircraft*, Vol. 24, No. 8, 1987, pp. 540-545.

12.   Madson, Michael D.: *Transonic Analysis of the F-16A with Under-Wing Fuel Tanks: An Application of the TranAir Full-Potential Code*. AIAA Paper 87-1198, 1987.

13.   Madson, Michael D.; Carmichael, Ralph L., and Mendoza, Joel P.: *Aerodynamic Analysis of Three Advanced Configurations Using the TranAir Full-Potential Code*. NASA CP-3020, Vol. 1, Part 2, 1989, pp. 437-452.

14. Goodsell, Aga M.; Madson, Michael D.; and Melton, John E.: *TranAir and Euler Computa tions of a Generic Fighter Including Comparisons with Experimental Data.* AIAA Paper 89-0263, 1989.

15. Johnson, Forrester T.; et. al.: *Application of the TranAir Rectangular Grid Approach to the Aerodynamic Analysis of Complex Configurations.* AGARD Specialists' Meeting on Applica tions of Mesh Generation to Complex 3-D Configurations, Loen, Norway, 1989.

16. Chen, A. W.; Curtin, M. M.; Carlson, R. B.; and Tinoco, E. N.: TRANAIR Applications to Engine/Airframe Integration. *AIAA J. Aircraft*, Vol. 27, No. 8, 1990, pp. 716-721.

17. Cenko, Alex; Tseng, Wei; Phillips, Kenneth, and Madson, Michael: *TranAir Applications to Transonic Flowfield Predictions.* AIAA Paper 91-0201, 1991.

18. Madson, Michael D.; and Erickson, Larry L.: Toward the Routine Aerodynamic Analysis of Complex Configurations. *Applied Computational Aerodynamics*, edited by P. A. Henne, AIAA Progress in Astronautics and Aeronautics, Vol. 125, 1990.

19. Thomas, Charles L.: *Extrapolation of Sonic Boom Pressure Signatures by the Waveform Pa rameter Method.* NASA TN D-6832, 1972.

20. Samant, Satish S.; et. al.: *TranAir: A Computer Code for Transonic Analyses of Arbitrary Configurations.* AIAA Paper 87-0034, 1987.

21. Rubbert, Paul E.; et. al.: A New Approach to the Solution of Boundary Value Problems In volving Complex Configurations. *Computational Mechanics – Advances and Trends*, pub lished by ASME, New York, 1986, p. 49.

22. Melvin, Robin G.; et. al.: *Local Grid Refinement for Transonic Flow Problems.* 6th Interna tional Conference on Numerical Methods in Laminar and Turbulent Flow, Swansea, U.K., 1989.

23. Bieterman, Michael B.; et. al.: Solution Adaptive Local Rectangular Grid Refinement for Tran sonic Aerodynamic Flow Problems. *8th GAMM Conference on Numerical Methods in Fluid Mechanics*, Delft, The Netherlands, 1989.

24. Hermstad, Dexter L.. *RAID User's Guide.* Sterling Federal Systems, Inc. Technical Note No. 33, Rev. 3, 1991.
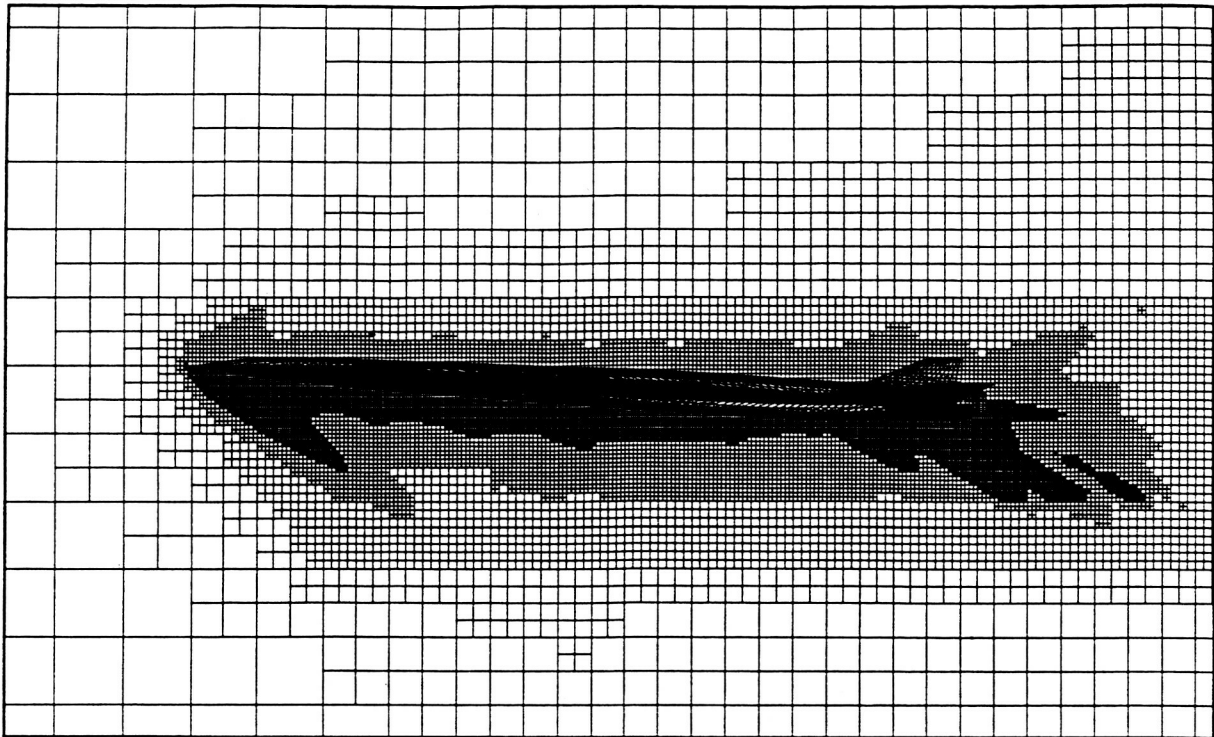
160 ft

300 ft

313 ft
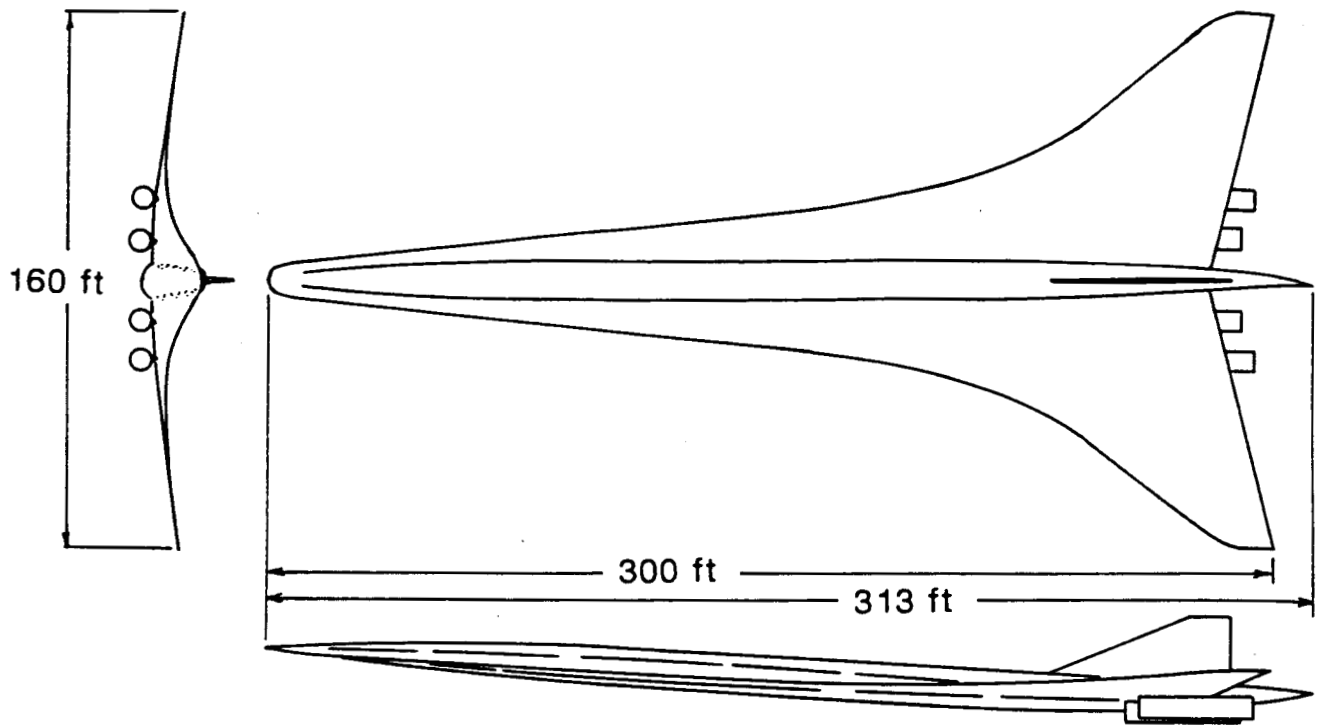
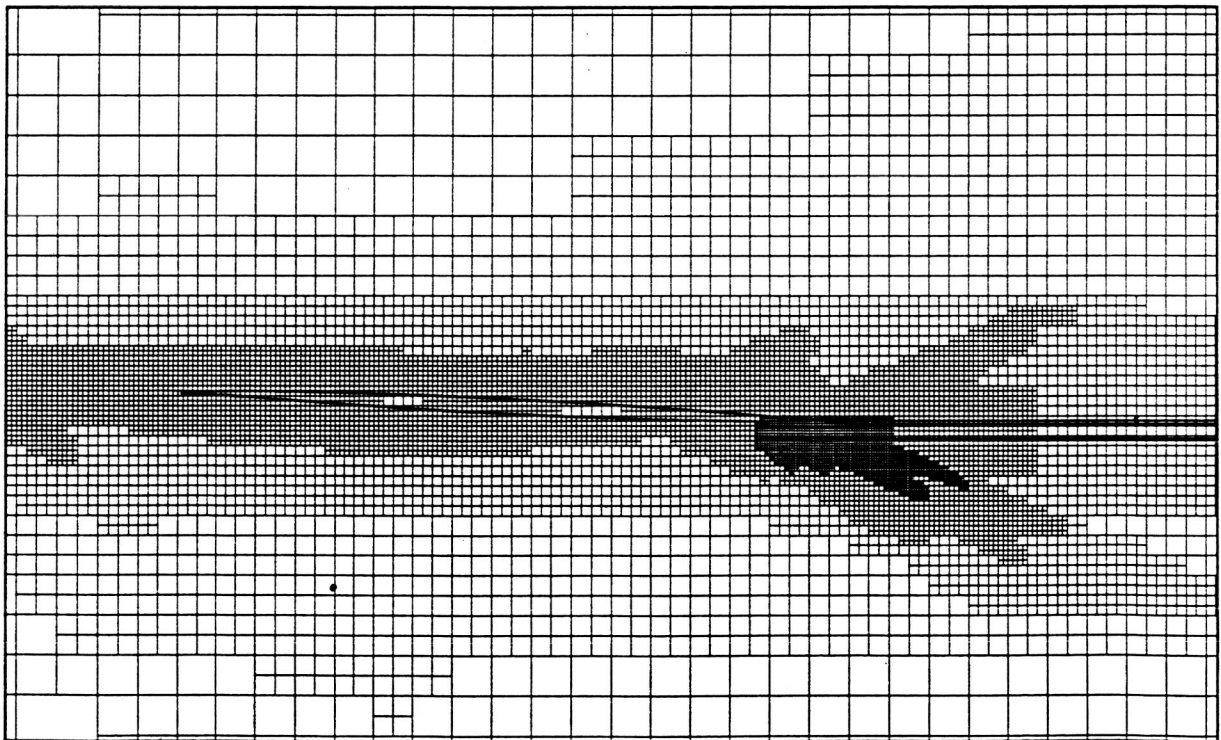1.   Three-view drawing of the Mach 2 model.
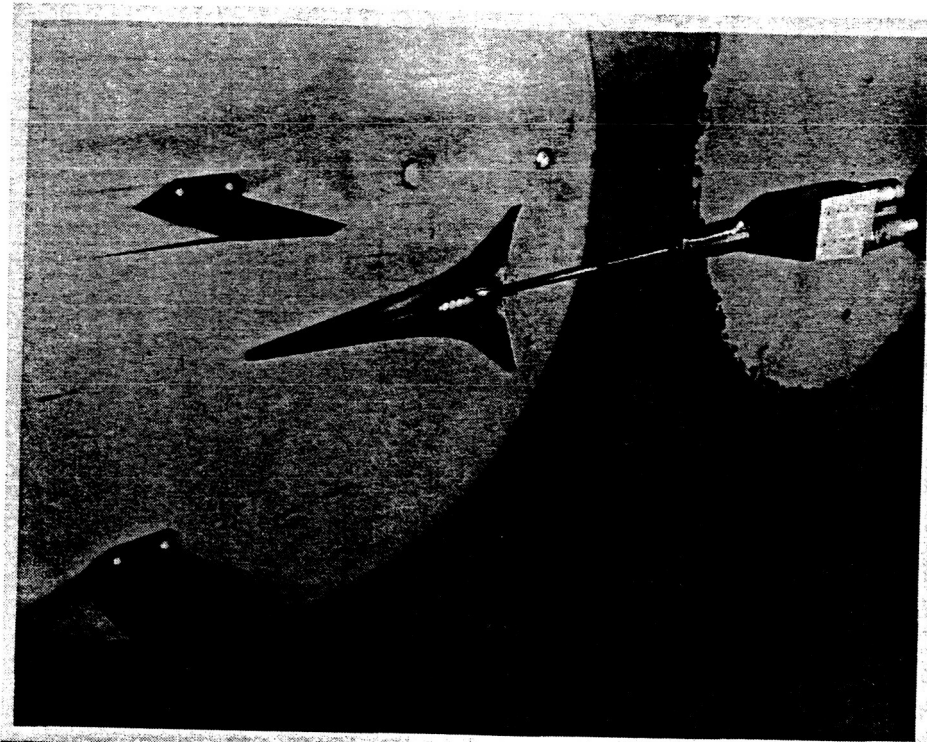
2. Mach 2 model installed in NASA Ames 9 ft by 7 ft supersonic wind tunnel.
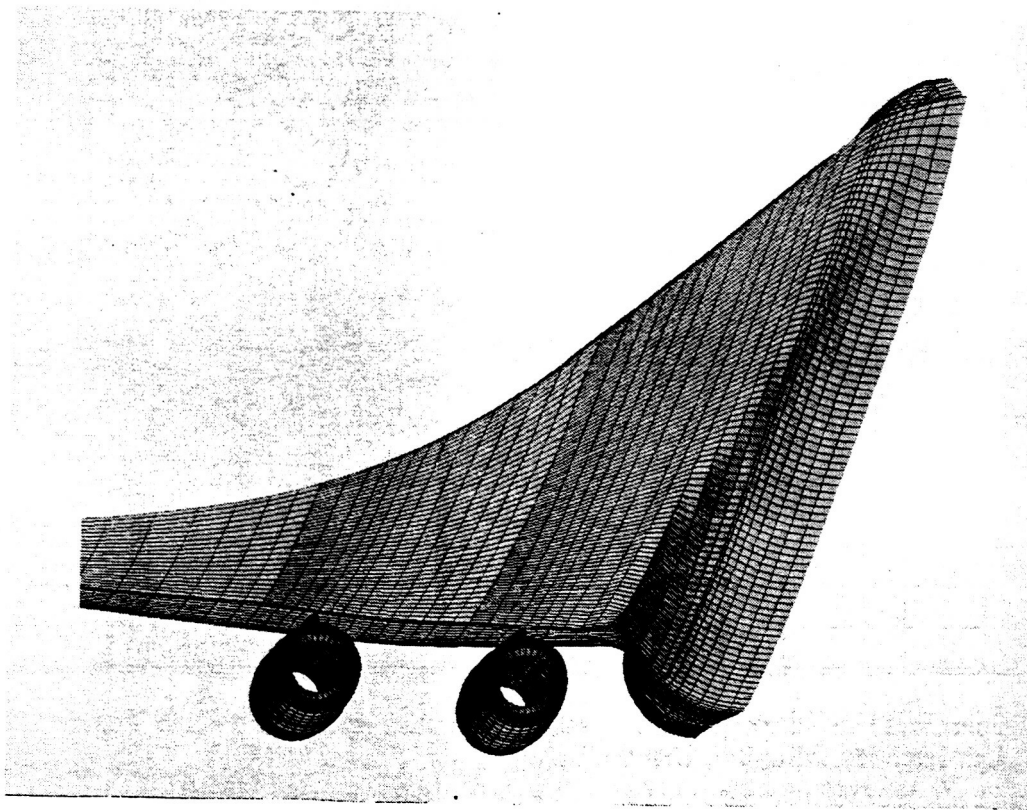
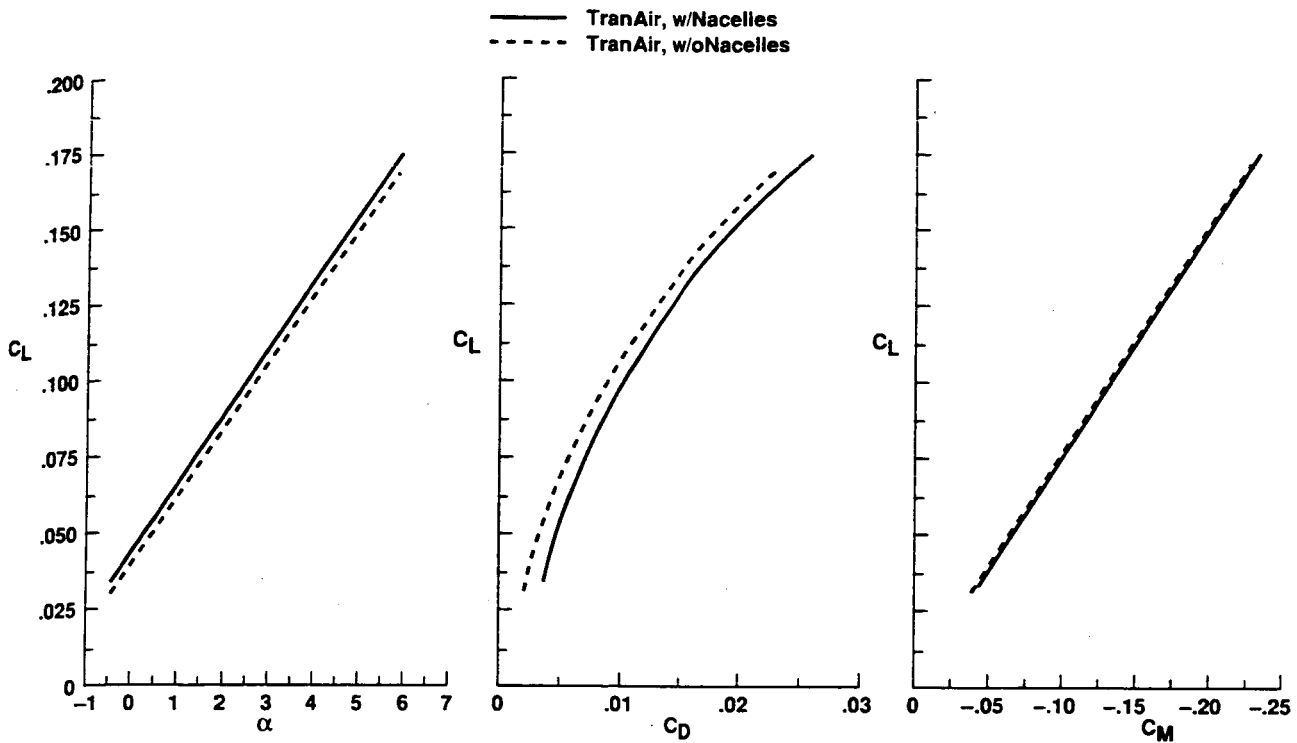3. TranAir surface-panel definition of the Mach 2 model with flow-through nacelles.
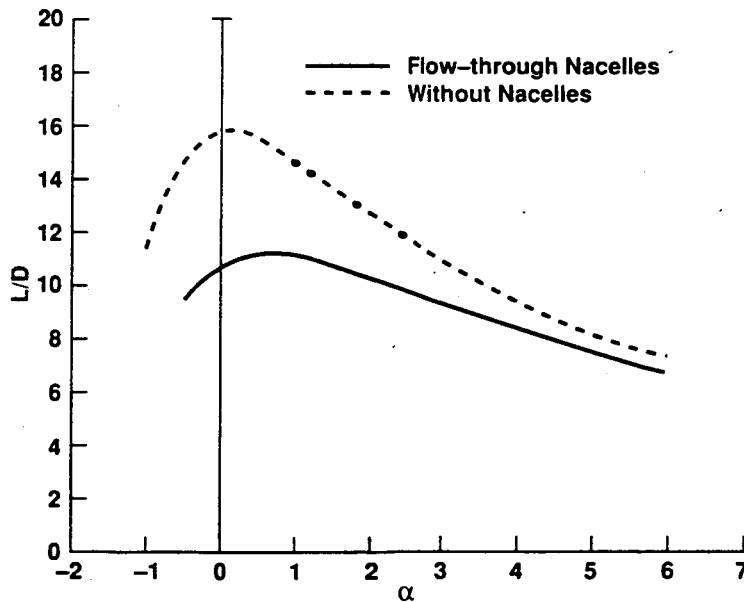
4. 2-Dimensional cuts through TranAir solution-adaptive grid for the Mach 2 model with flow-through nacelles, $M_\infty=2.0$, $C_N=0.07$.

a. Centerplane.
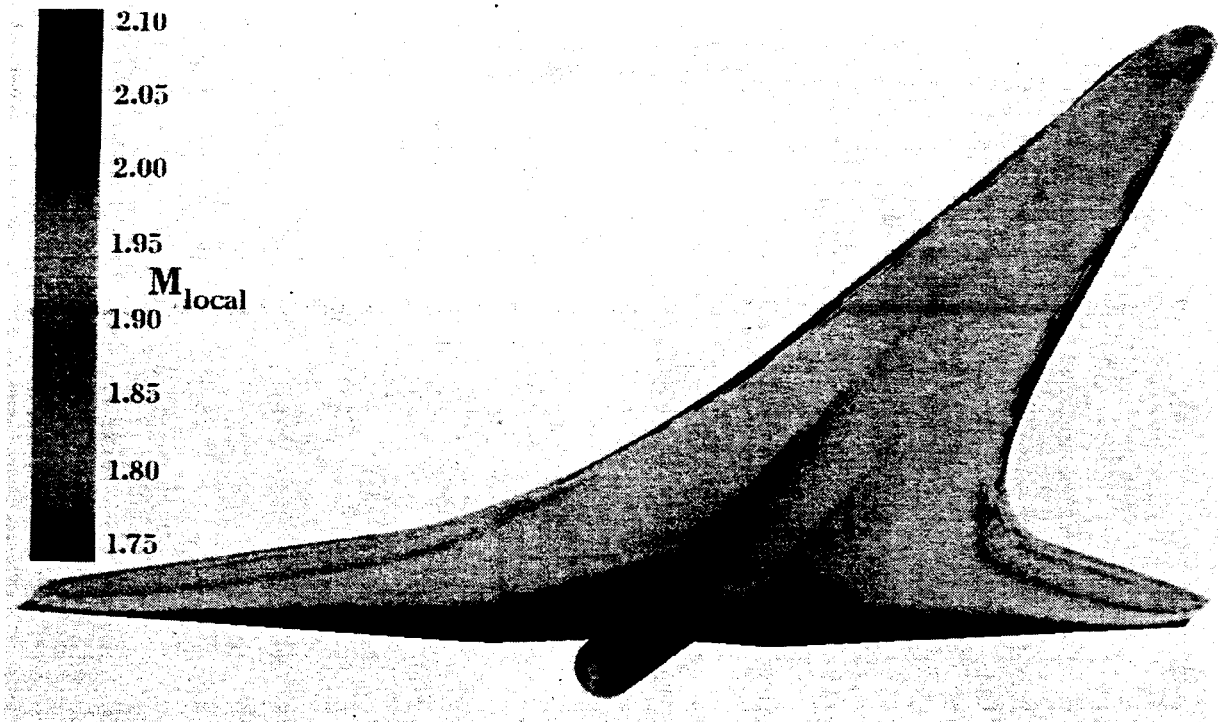b. Through wing and centerline of inboard nacelle.

5. TranAir force and moment predictions for the Mach 2 model with and without nacelles, M_∞=2.0.

    a.Lift vs. angle of attack
    b.Lift vs. drag
    c.Lift vs. pitching moment

6. TranAir L/D predictions for the Mach 2 model with and without nacelles, M_∞=2.0.

7. Mach contours for the Mach 2 model without nacelles, M_∞=2.0, C_N=0.05.
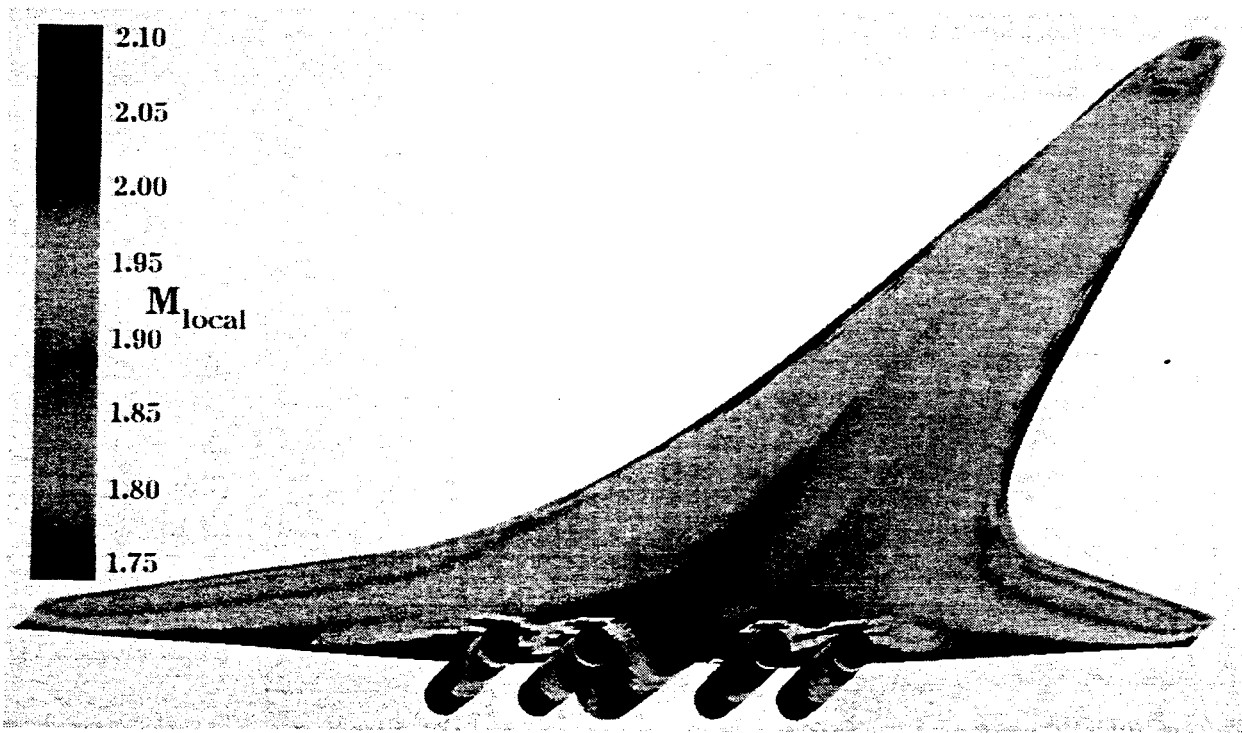
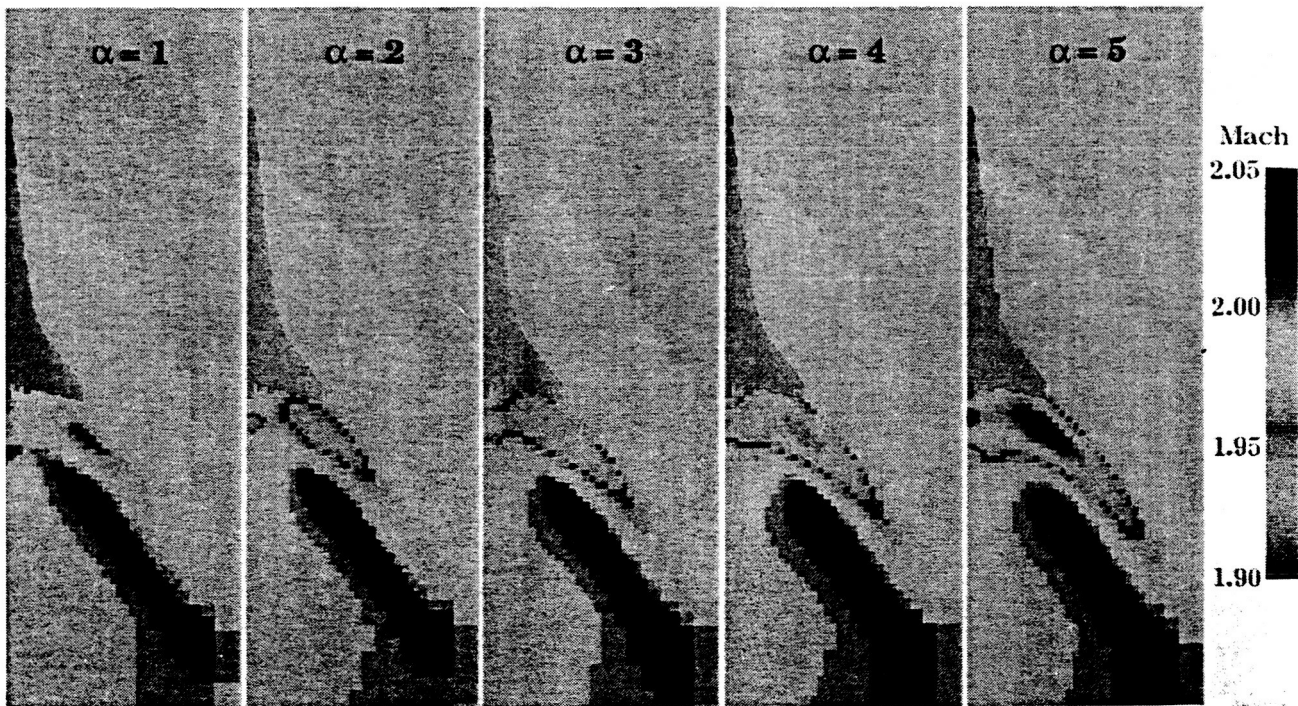8. Mach contours for the Mach 2 model with flow-through nacelles, M_∞=2.0, C_N=0.05.
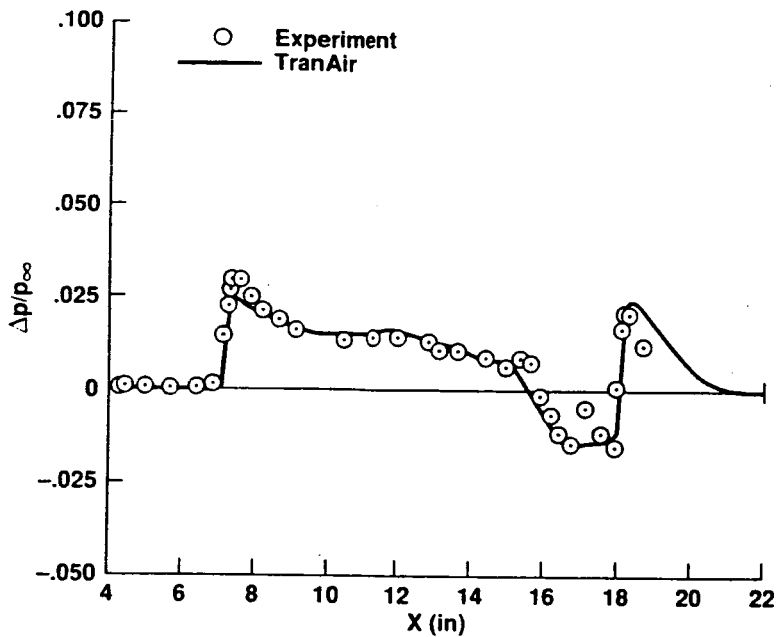
9. Pressure signature comparisons on ground-track for the Mach 2 model without nacelles, h/L=0.651, M_∞=2.0, C_N=0.05.
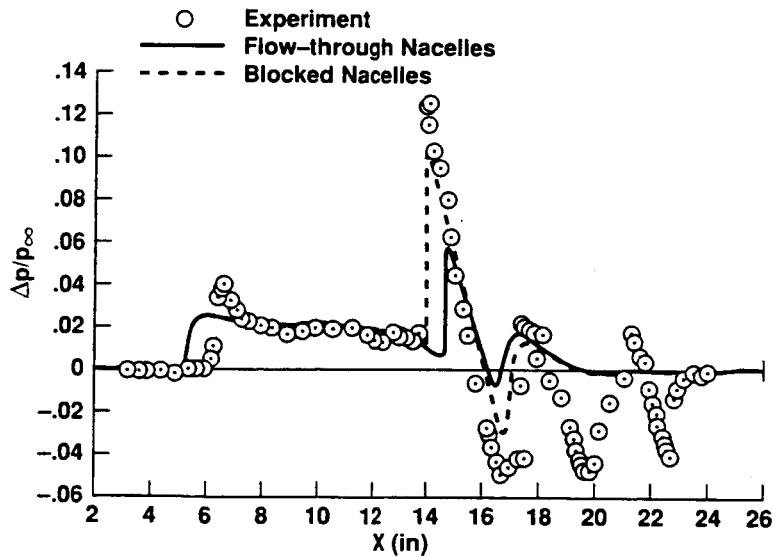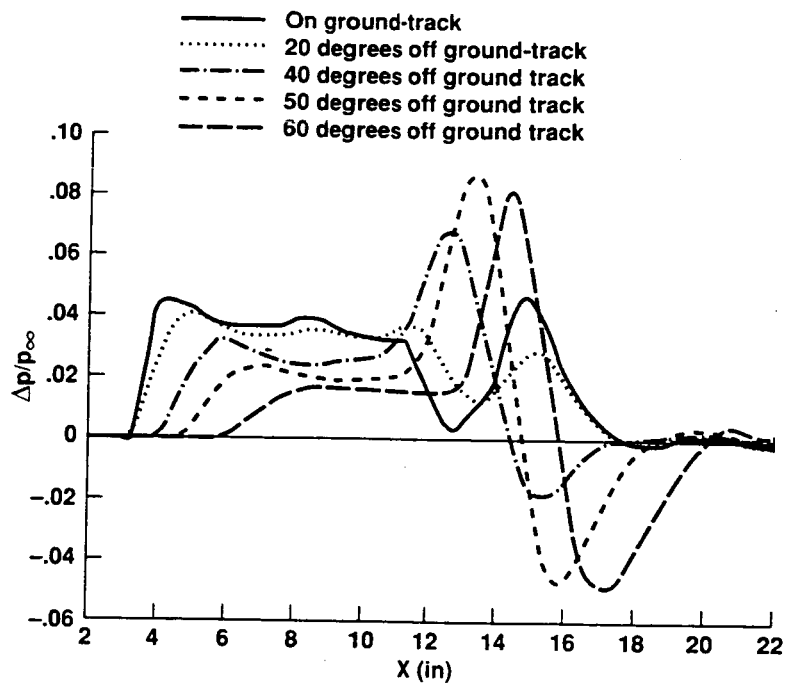

10. Pressure signature comparisons on ground-track for the Mach 2 model with flow-through nacelles, h/L=0.651, M_∞=2.0, C_N=0.07.
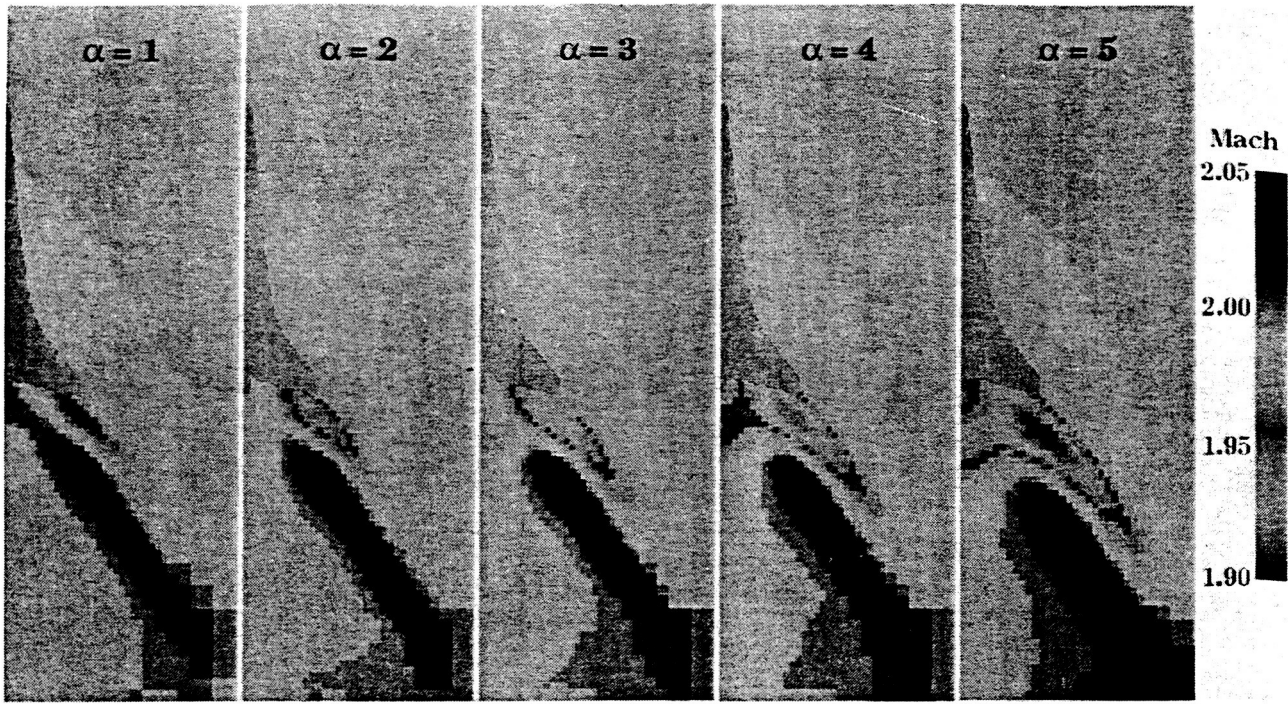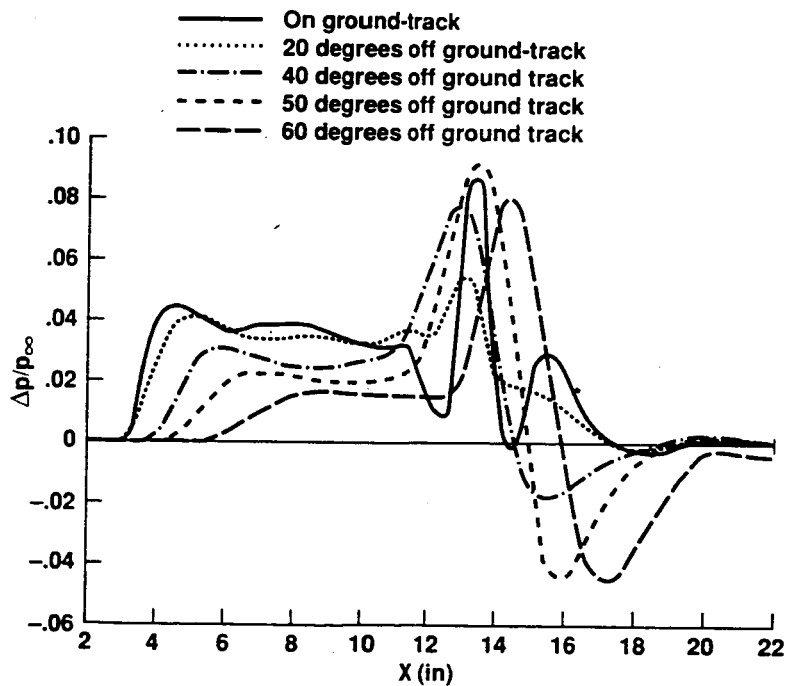
11. TranAir sonic boom footprints for the Mach 2 model without nacelles, h/L=0.20, M∞=2.0.

12. TranAir sonic boom footprints for the Mach 2 model with flow-through nacelles, h/L=0.20, M∞=2.0.

172

13. TranAir off ground-track pressure signature comparisons for the Mach 2 model without nacelles, h/L=0.20, M_∞=2.0, C_N=0.08.

14. TranAir off ground-track pressure signature comparisons for the Mach 2 model with flow-through nacelles, h/L=0.20, M_∞=2.0, C_N=0.08.